Journal of Engineering Mathematics **33:** 61–76, 1998.

High-Reynolds-number flow about a submerged circular cylinder induced by free-surface travelling waves on finite depth

B. YAN[1], N. AMIN[2] and N. RILEY[1]
[1]*School of Mathematics, University of East Anglia, Norwich, NR4 7TJ, United Kingdom*
[2]*Jabatan Matematik, Universiti Teknologi Malaysia, 80990 Johor Bahru, Malaysia*

Received 27 November 1996; accepted in revised form 30 July 1997

Abstract. We consider the fluid flow induced when free-surface travelling waves, on fluid whose depth is finite and uniform in its undisturbed state, pass over a submerged circular cylinder. The wave amplitude is assumed to be small, and a suitably defined Reynolds number large. Thus, the inviscid flow may be pursued by perturbation methods, as may viscous effects that are confined to thin boundary layers on the cylinder and bed beneath it. Particular attention is focused on the steady streaming motion, which induces a circulation about the cylinder. The consequences of this on bed scouring beneath the cylinder, when the bed is erodible, are considered.

Key words: surface waves, free surface, Reynolds number, circular cylinder, boundary layer.

1. Introduction

In this paper we consider the flow induced about a circular cylinder, in a high-Reynolds number flow, when plane waves propagate over a free surface below which the cylinder is located. The wave crests are parallel to the cylinder, and the fluid is of finite depth, see Figure 1. The work is an extension of earlier work by Wybrow, Yan and Riley [1], Wybrow and Riley [2] and in particular by Riley and Yan [3], and Yan and Riley [4]. In [1, 2] the flow about a cylinder located beneath standing waves when the cylinder is located above the bed [1], as in Figure 1, or partially embedded within it [2], is considered. In [3, 4] the case of progressive waves is considered, when the fluid is of infinite depth for both inviscid [3] and viscous [4] flow. In spite of the suggestion made in [1] the present investigation has more in common with [3, 4], and not least because we again find that there is circulation about the cylinder. The final flow structures that we predict suggest that, if the bed beneath the cylinder is erodible, then material will be scoured from it immediately below the cylinder.

In Section 2 we introduce the governing equations and immediately, in Section 2.1, we attack them in the inviscid-flow limit. As in [3] the solution is developed as a series in powers of the dimensionless amplitude of the incident waves. For the case of infinite depth it has long been known, [5, 6], that there is no reflected wave at leading order, a result that has been extended to second order by McIver and McIver [7]. In the present case we find the reflected wave at leading order; but at second order we focus our attention upon only the time-averaged part of the solution since it is the steady streaming that is our prime concern with reference, in particular, to bed scouring. As in [3] the time-averaged inviscid flow cannot be determined uniquely; a solution with arbitrary circulation about the cylinder may always be added. The circulation about the cylinder is determined from a consideration of viscous effects in Section 2.2. For a fluid of small viscosity, viscous effects at the solid boundaries are confined, at leading order, to a thin Stokes shear-wave layer. It is within the Stokes layer that the Reynolds stresses act to generate an additional element of time-averaged flow. This

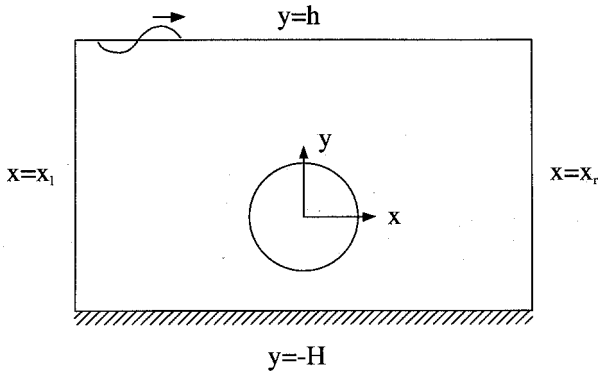

Figure 1. Definition sketch.

persists beyond the Stokes layer where an outer boundary layer is required if a proper match with the outer, inviscid, time-averaged flow is to be effected. It is this matching between the viscous boundary layer flow and inviscid outer flow that determines the unique circulation about the cylinder. With the outer inviscid flow now determined, the viscous boundary layer at the bed may be addressed. As at the cylinder surface it exhibits a double structure.

In Section 3 we describe, briefly, the numerical techniques used; for more detail of this reference may be made to [4]. In Section 4 we discuss the results obtained, with particular reference to the time-averaged features of the flow. For the case of infinite depth [3, 4] two parameters, namely cylinder depth h and wave number k, both made dimensionless with cylinder radius a as in (1), were involved to which we now can add the overall fluid depth as a third. Because of the considerable computational effort involved we have restricted our attention to cases for which $k = 0{\cdot}5$. The main features of the time-averaged flow are the free-surface elevation, which takes the form of a small-amplitude stationary wave ahead of the cylinder, but is virtually uniform behind it, and the circulation about the cylinder which owes its origins to viscous effects. As the gap between the cylinder and bed decreases so too, of course, does this circulation, vanishing in the limit. The boundary-layer structure at the bed is of particular interest, since the dynamics of the flow there is responsible for the transport of any bed material if the bed is erodible. In the absence of any turbulent fluctuations in our assumed laminar flow, we argue that shear-induced diffusion will levitate particles from the bed which are then transported in the outer streaming boundary layer. Such mechanisms are shown to result in net scouring of the bed immediately beneath the cylinder.

2. Governing equations

We consider the flow induced when two-dimensional waves propagate at the surface of an almost inviscid, incompressible fluid over a circular cylinder of radius a. The wave crests are parallel to the cylinder generators. The centre of the cylinder is at depth h' beneath the mean position of the free surface, and at height H' above the bed, so that the mean fluid depth is $h' + H'$. The waves have wave number k', frequency ω', and amplitude A. We define dimensionless quantities as follows

$$\left.\begin{aligned} &x = x'/a, \quad y = y'/a, \quad h = h'/a, \quad H = H'/a, \quad \epsilon = A/a, \\ &k = k'a, \quad t = \omega' t', \quad \eta = \eta'/a, \quad \phi = \phi'/\omega' a^2, \quad \psi = \psi'/\omega' a^2, \quad \mathbf{v} = \mathbf{v}'/\omega' a. \end{aligned}\right\} \tag{1}$$

In Equations (1) x', y' are Cartesian co-ordinates whose origin is at the centre of the cylinder with y' measured vertically upwards, t' is time, η' is the free-surface elevation above $y' = h'$, ϕ' is a velocity potential, $\mathbf{v}' = (v_r', v_\theta')$ is the velocity vector, and ψ' is the stream function. The dimensionless velocity components and stream function are related by

$$v_r = r^{-1}\frac{\partial \psi}{\partial \theta}, \qquad v_\theta = -\frac{\partial \psi}{\partial r}.$$

The non-dimensional equation for the stream function ψ derived from the two-dimensional Navier–Stokes equations may be written, in terms of $polar$ co-ordinates r, θ whose origin is also at the centre of the cylinder with $\theta = 0$ coincident with the direction of propagation of the incident waves, as

$$\frac{\partial(\nabla^2\psi)}{\partial t} - \frac{1}{r}\frac{\partial(\psi, \nabla^2\psi)}{\partial(r,\theta)} = \frac{\epsilon^2}{R_s}\nabla^4\psi, \tag{2}$$

which is to be solved subject to no-slip conditions at solid boundaries, and suitable conditions at the free surface. We note from (2) that the flow is characterised by two parameters namely ϵ, and the so-called streaming Reynolds number

$$R_s = \frac{A^2\omega'}{\nu}. \tag{3}$$

Our interest is in cases for which $\epsilon \ll 1$, with $R_s = O(1)$, formally $\lim_{\epsilon\to 0} R_s = O(1)$, and a double-limit procedure allows us, subsequently, to take $R_s \gg 1$. For $\epsilon \ll 1$ the right-hand side of (2) is negligible and the flow is largely inviscid, except of course close to solid boundaries where viscous effects become important in thin boundary layers.

It proves convenient, as is usual in such situations, to consider the inviscid, and boundary-layer, flows separately.

2.1. INVISCID FLOW

With viscous effects ignored the flow is irrotational so that $\nabla^2\psi = 0$. However for an irrotational flow with a free surface it is more convenient to work with the velocity potential ϕ, related to the stream function by the Cauchy–Riemann equations

$$\frac{\partial \psi}{\partial x} = -\frac{\partial \phi}{\partial y}, \qquad \frac{\partial \psi}{\partial y} = \frac{\partial \phi}{\partial x}.$$

The potential ϕ also satisfies the Laplace equation

$$\nabla^2\phi = 0, \tag{4}$$

together with $\partial\phi/\partial n = 0$ at a solid boundary, where **n** is the unit normal to the boundary, and conditions at the free surface, derived from the kinematic and dynamic boundary conditions at the free surface $\eta = \eta(x,t)$ as

$$\frac{\partial \eta}{\partial t} + \frac{\partial \phi}{\partial x}\frac{\partial \eta}{\partial x} = \frac{\partial \phi}{\partial y}, \tag{5}$$

$$\eta(x,t) = -\Omega\left[\frac{\partial\phi}{\partial t} + \frac{1}{2}\left\{\left(\frac{\partial\phi}{\partial x}\right)^2 + \left(\frac{\partial\phi}{\partial y}\right)^2\right\}\right], \tag{6}$$

where $\Omega = a\omega'^2/g$.

With $\epsilon \ll 1$ we expand ϕ and η as

$$\phi = \epsilon\phi_1 + \epsilon^2\phi_2 + \cdots, \qquad \eta = \epsilon\eta_1 + \epsilon^2\eta_2 + \cdots. \tag{7, 8}$$

From (7) and (4) we see that each term ϕ_i satisfies Laplace's equation. The free-surface conditions are however nonlinear, and are applied at a location that is not pre-determined. With the expansions (7) and (8) substituted in (5) and (6), we transfer the boundary condition from its exact location at the free surface to its mean position $y = h$ by expanding the potential and its derivatives as Taylor series. Coefficients of like powers of ϵ then yield boundary conditions for the successive terms of our expansions as

$$\eta_1 = -\Omega\frac{\partial\phi_1}{\partial t}, \quad \eta_2 = -\Omega\left[\frac{\partial\phi_2}{\partial t} - \Omega\frac{\partial\phi_1}{\partial t}\frac{\partial^2\phi_1}{\partial y\partial t} + \frac{1}{2}\left\{\left(\frac{\partial\phi_1}{\partial x}\right)^2 + \left(\frac{\partial\phi_1}{\partial y}\right)^2\right\}\right], \tag{9, 10}$$

$$\Omega\frac{\partial^2\phi_1}{\partial t^2} + \frac{\partial\phi_1}{\partial y} = 0, \tag{11}$$

$$\Omega\frac{\partial^2\phi_2}{\partial t^2} + \frac{\partial\phi_2}{\partial y} = \Omega\frac{\partial\phi_1}{\partial t}\left(\Omega\frac{\partial^3\phi_1}{\partial y\partial t^2} + \frac{\partial^2\phi_1}{\partial y^2}\right) - 2\Omega\left(\frac{\partial\phi_1}{\partial x}\frac{\partial^2\phi_1}{\partial x\partial t} + \frac{\partial\phi_1}{\partial y}\frac{\partial^2\phi_1}{\partial y\partial t}\right). \tag{12}$$

All terms in (9) to (12) are now evaluated at $y = h$, and in deriving (11), (12) use has been made of (9) and (10) to eliminate η_1 and η_2.

We now write ϕ_1, ϕ_2 as

$$\phi_1 = \overline{\phi}_{11}\cos t + \overline{\phi}_{12}\sin t = (\phi_{01} + \phi_{11})\cos t + (\phi_{02} + \phi_{12})\sin t, \tag{13}$$

$$\phi_2 = \phi_{20} + \phi_{21}\cos 2t + \phi_{22}\sin 2t, \tag{14}$$

where $\phi_{ij} = \phi_{ij}(x,y)$. In equation (13) the incident wave is given by

$$\phi_{01}\cos t + \phi_{02}\sin t = -\frac{\cosh\{k(y+H)\}\cos(kx - t)}{k\sinh\{k(h+H)\}} = \phi_0, \quad \text{say}, \tag{15}$$

and we see that (15) satisfies (11), provided that

$$\Omega = k\tanh k(h+H). \tag{16}$$

As we have already indicated it is the steady streaming induced at second order that is our main concern, since it is this which is responsible for the bed-scouring beneath the cylinder. As a consequence we need to determine only ϕ_{11}, ϕ_{12} and ϕ_{20} in equations (13) and (14). The unknowns $\phi_{11}, \phi_{12}, \phi_{20}$ satisfy

$$\nabla^2\phi_{11} = \nabla^2\phi_{12} = \nabla^2\phi_{20} = 0$$

together with

$$\frac{\partial \phi_{1j}}{\partial y} = \Omega \phi_{1j}, \quad \text{at } y = h, \quad j = 1, 2, \tag{17}$$

$$\frac{\partial \phi_{20}}{\partial y} = -\frac{\Omega}{2}\left(\frac{\partial^2 \overline{\phi}_{11}}{\partial x^2}\overline{\phi}_{12} - \frac{\partial^2 \overline{\phi}_{12}}{\partial x^2}\overline{\phi}_{11} \right), \quad \text{at } y = h, \tag{18}$$

$$\frac{\partial \phi_{1j}}{\partial y} = \frac{\partial \phi_{20}}{\partial y} = 0, \quad \text{at } y = -H, \quad j = 1, 2, \tag{19}$$

$$\frac{\partial \phi_{1j}}{\partial r} = -\frac{\partial \phi_{0j}}{\partial r}, \qquad \frac{\partial \phi_{20}}{\partial r} = 0, \quad \text{at } r = 1, \quad j = 1, 2, \tag{20}$$

$$\frac{\partial \phi_{11}}{\partial x} + k\phi_{12}, \qquad \frac{\partial \phi_{12}}{\partial x} - k\phi_{11}, \qquad \frac{\partial \phi_{20}}{\partial x} \to 0 \quad \text{as } x \to +\infty, \tag{21}$$

$$\frac{\partial \phi_{11}}{\partial x} - k\phi_{12}, \qquad \frac{\partial \phi_{12}}{\partial x} + k\phi_{11}, \qquad \frac{\partial \phi_{20}}{\partial x} \to 0 \quad \text{as } x \to -\infty, \tag{22}$$

where the conditions (21), (22) for ϕ_{11}, ϕ_{12} are the radiation conditions; the conditions for ϕ_{20} as $x \to \pm\infty$ reflect the fact that the mean second order potential is localised to its origin, namely the cylinder.

The conditions for ϕ_{20} set out in (18) to (22) do not determine ϕ_{20} uniquely. To this time-independent part of the solution we may add the potential of a line vortex located within the circular cylinder, which introduces a circulation about it. As in other branches of fluid dynamics, notably wing theory, the circulation can only be fixed by a consideration of viscous effects, and we return to this point in the next subsection.

Finally, we have the free surface given by

$$\eta(x, t) = \epsilon(\eta_{11} \cos t + \eta_{12} \sin t) + \epsilon^2(\eta_{20} + \eta_{21} \cos 2t + \eta_{22} \sin 2t) + \cdots, \tag{23}$$

where

$$\eta_{11} = \sin kx - \Omega\phi_{12}|_{y=h}, \qquad \eta_{12} = -\cos kx + \Omega\phi_{11}|_{y=h}, \tag{24}$$

and

$$\eta_{20} = -\frac{1}{4}\Omega \left\{ \left(\frac{\partial \overline{\phi}_{11}}{\partial x} \right)^2 + \left(\frac{\partial \overline{\phi}_{12}}{\partial x} \right)^2 - \Omega^2(\overline{\phi}_{11}^2 + \overline{\phi}_{12}^2) \right\}_{y=h}. \tag{25}$$

2.2. VISCOUS EFFECTS

Here we work with the stream function ψ, which we expand in a manner analogous to (7) as

$$\psi(\mathbf{x}, t) = \epsilon\psi_1(\mathbf{x}, t) + \epsilon^2\{\psi_{20}(\mathbf{x}) + \psi_{21}(\mathbf{x}, t)\} + \epsilon^3\psi_3(\mathbf{x}, t) + \epsilon^4\psi_4(\mathbf{x}, t) \ldots, \tag{26}$$

where at $O(\epsilon^2)$ we have again acknowledged the presence of a non-zero time-averaged contribution, namely ψ_{20}, which is our main concern. Substituting (26) in (2) gives, at leading order,

$$\frac{\partial(\nabla^2\psi_1)}{\partial t} = 0. \tag{27}$$

The solution for ψ_1 may be inferred directly from ϕ_1 via the Cauchy–Riemann equations. This inviscid solution does not satisfy the no-slip condition at either the cylinder surface or the bed $y = -H$. At each of these a boundary layer, the classical Stokes layer of thickness $O(\nu/\omega)^{1/2}$ is required. We detail only the boundary layer on the cylinder and summarise the analogous results on the bed, as required. For the boundary layer on the cylinder we introduce the variables

$$\Psi = \frac{R_s^{1/2}\psi}{\sqrt{2}\epsilon}, \qquad \rho = \frac{R_s^{1/2}(r-1)}{\sqrt{2}\epsilon}, \tag{28}$$

and expand Ψ as

$$\Psi = \epsilon\Psi_1(\rho,\theta,t) + \epsilon^2\{\Psi_{20}(\rho,\theta) + \Psi_{21}(\rho,\theta,t)\} + \cdots. \tag{29}$$

Substitution (29) in the Stokes-layer equation gives, at leading order,

$$\frac{\partial}{\partial t}\left(\frac{\partial^2\Psi_1}{\partial\rho^2}\right) = \frac{1}{2}\frac{\partial^4\Psi_1}{\partial\rho^4}. \tag{30}$$

The solution of (30) with $\Psi_1 = \partial\Psi_1/\partial\rho = 0$ at $\rho = 0$ is

$$\Psi_1 = c_1(\theta)(e^{\gamma_1\rho} - \gamma_1\rho - 1)e^{it}, \tag{31}$$

where $\gamma_1 = -1 - i$, and $c_1(\theta) = c_{11}(\theta) - ic_{12}(\theta)$ is to be determined; the real part of any complex quantity is to be understood. We determine the unknown $c_1(\theta)$ by matching with the outer solution which requires

$$\lim_{\rho\to\infty}\frac{\partial\Psi_1}{\partial\rho} = \left.\frac{\partial\psi_1}{\partial r}\right|_{r=1}. \tag{32}$$

As with the velocity potential, it proves convenient to write

$$\psi_1 = \psi_{11}(r,\theta)\cos\,t + \psi_{12}(r,\theta)\sin\,t, \quad \Psi_1 = \Psi_{11}(\rho,\theta)\cos\,t + \Psi_{12}(\rho,\theta)\sin\,t, \tag{33}$$

and matching gives

$$c_{11} = \frac{1}{2}\left(\frac{\partial\psi_{11}}{\partial r} - \frac{\partial\psi_{12}}{\partial r}\right)_{r=1}, \qquad c_{12} = \frac{1}{2}\left(\frac{\partial\psi_{11}}{\partial r} + \frac{\partial\psi_{12}}{\partial r}\right)_{r=1}. \tag{34}$$

We consider next the steady streaming, which is of most concern to us, and represented by Ψ_{20} in (29) which satisfies

$$\frac{1}{2}\frac{\partial^4\Psi_{20}}{\partial\rho^4} = \left\langle\left(\frac{\partial\Psi_1}{\partial\theta}\frac{\partial^3\Psi_1}{\partial\rho^3} - \frac{\partial\Psi_1}{\partial\rho}\frac{\partial^3\Psi_1}{\partial\rho^2\partial\theta}\right)\right\rangle, \tag{35}$$

where, in (35), $\langle\cdot\rangle$ denotes a time average. The solution of (35) that satisfies $\Psi_{20} = \partial\Psi_{20}/\partial\rho = 0$ at $\rho = 0$, with $\partial\Psi_{20}/\partial\rho$ bounded as $\rho \to \infty$, is

$$\begin{aligned}\Psi_{20} \;=\; & (c_{11}c'_{12} - c_{12}c'_{11})(\tfrac{1}{4}\,\mathrm{e}^{-2\rho} - \rho\,\mathrm{e}^{-\rho}\cos\,\rho + 2\,\mathrm{e}^{-\rho}\sin\,\rho - \mathrm{e}^{-\rho}\cos\,\rho)\\ & +(c_{11}c'_{11} + c_{12}c'_{12})(\tfrac{1}{4}\,\mathrm{e}^{-2\rho} + 3e^{-\rho}\cos\,\rho + \rho\,\mathrm{e}^{-\rho}\sin\,\rho + 2e^{-\rho}\sin\,\rho)\\ & +c_{20}(\theta)\rho + c_{21}(\theta),\end{aligned} \tag{36}$$

where

$$\begin{aligned}c_{20}(\theta) \;&=\; \tfrac{3}{2}(-c_{11}c'_{12} + c_{12}c'_{11} + c_{11}c'_{11} + c_{12}c'_{12})\\ &=\; \frac{3}{4}\left\{\frac{\partial\psi_{11}}{\partial r}\left(\frac{\partial^2\psi_{11}}{\partial r\partial\theta} - \frac{\partial^2\psi_{12}}{\partial r\partial\theta}\right) + \frac{\partial\psi_{12}}{\partial r}\left(\frac{\partial^2\psi_{11}}{\partial r\partial\theta} + \frac{\partial^2\psi_{12}}{\partial r\partial\theta}\right)\right\}_{r=1},\end{aligned} \tag{37}$$

$$\begin{aligned}c_{21}(\theta) \;&=\; \tfrac{3}{4}(c_{11}c'_{12} - c_{12}c'_{11}) - \tfrac{13}{4}(c_{11}c'_{11} + c_{12}c'_{12})\\ &=\; \left\{-\frac{13}{8}\left(\frac{\partial\psi_{11}}{\partial r}\frac{\partial^2\psi_{11}}{\partial r\partial\theta} + \frac{\partial\psi_{12}}{\partial r}\frac{\partial^2\psi_{12}}{\partial r\partial\theta}\right) + \frac{3}{8}\left(\frac{\partial\psi_{11}}{\partial r}\frac{\partial^2\psi_{12}}{\partial r\partial\theta} - \frac{\partial\psi_{12}}{\partial r}\frac{\partial^2\psi_{11}}{\partial r\partial\theta}\right)\right\}_{r=1},\end{aligned} \tag{38}$$

and a prime denotes differentiation with respect to θ.

We note that $c_{20}(\theta)$ is uniquely determined by (37), and that there is no choice of the circulation in the outer inviscid flow, discussed in section 2.1 above, which will allow the Stokes-layer solution (36) to match directly with it. For $R_s \gg 1$, which is the case we consider in detail, an outer boundary layer is required for the transition from the Stokes layer to the outer inviscid flow.

To continue, we substitute (26) in (2), and then from the terms at $O(\epsilon^2), O(\epsilon^3), O(\epsilon^4)$ we find, respectively,

$$\frac{\partial(\nabla^2\psi_{21})}{\partial t} = 0, \tag{39}$$

$$\frac{\partial}{\partial t}(\nabla^2\psi_3) = \frac{1}{r}\frac{\partial(\psi_1, \nabla^2\psi_{20})}{\partial(r,\theta)} = \frac{1}{r}\left\{\frac{\partial(\psi_{11}, \nabla^2\psi_{20})}{\partial(r,\theta)}\cos\,t + \frac{\partial(\psi_{12}, \nabla^2\psi_{20})}{\partial(r,\theta)}\sin\,t\right\}, \tag{40}$$

$$\frac{1}{R_s}\nabla^4\psi_{20} = \frac{1}{r}\left\{\frac{\partial(\nabla^2\psi_{20}, \psi_{20})}{\partial(r,\theta)} + \left\langle\frac{\partial(\nabla^2\psi_3, \psi_1)}{\partial(r,\theta)}\right\rangle\right\}, \tag{41}$$

where (41) has, in fact, been derived from the equation at $O(\epsilon^4)$ by taking a time average. Our prime concern is with the steady streaming ψ_{20}, and to determine an equation for this we must eliminate ψ_3 from Equations (40) and (41). First, we integrate (40) with respect to t, to give

$$\nabla^2\psi_3 = \frac{1}{r}\left\{\frac{\partial(\nabla^2\psi_{20}, \psi_{12})}{\partial(r,\theta)}\cos\,t - \frac{\partial(\nabla^2\psi_{20}, \psi_{11})}{\partial(r,\theta)}\sin\,t\right\} + \tilde{\chi}(r,\theta), \tag{42}$$

where $\tilde{\chi}(r,\theta)$ is an unknown function of r and θ only. Using this result we may, following considerable manipulation, eliminate ψ_3 from (41) and write

$$\left\langle \frac{1}{r}\frac{\partial(\nabla^2\psi_3,\psi_1)}{\partial(r,\theta)} \right\rangle = V_r^d \frac{\partial(\nabla^2\psi_{20})}{\partial r} + \frac{V_\theta^d}{r}\frac{\partial(\nabla^2\psi_{20})}{\partial\theta}. \tag{43}$$

In Equation (43) V_r^d, V_θ^d are the $r-$ and $\theta-$components of the Stokes drift velocity defined as

$$\mathbf{V}^d = \left\langle \left(\int^t \mathbf{v}_1 \,\mathrm{d}t.\nabla \right) \mathbf{v}_1 \right\rangle, \tag{44}$$

where $\mathbf{v}_1 = (r^{-1}\partial\psi_1/\partial\theta, -\partial\psi_1/\partial r)$ is determined from the first-order solution. With $R_s \gg 1$ in Equation (41) the viscous flow outside the Stokes layer is itself of boundary-layer character and so we only require the form of $\mathbf{V}^d$ close to the boundary. And we write

$$V_r^d = \left.\frac{\partial V_r^d}{\partial r}\right|_{r=1}(r-1)+\cdots, \qquad V_\theta^d = \left.V_\theta^d\right|_{r=1} + \left.\frac{\partial V_\theta^d}{\partial r}\right|_{r=1}(r-1)+\cdots, \tag{45}$$

where

$$\left.\frac{\partial V_r^d}{\partial r}\right|_{r=1} = \frac{1}{2}\left(\frac{\partial\psi_{12}}{\partial r}\frac{\partial^3\psi_{11}}{\partial r\partial\theta^2} - \frac{\partial\psi_{11}}{\partial r}\frac{\partial^3\psi_{12}}{\partial r\partial\theta^2}\right)_{r=1}, \tag{46}$$

$$\left.V_\theta^d\right|_{r=1} = \frac{1}{2}\left(\frac{\partial\psi_{11}}{\partial r}\frac{\partial^2\psi_{12}}{\partial r\partial\theta} - \frac{\partial\psi_{12}}{\partial r}\frac{\partial^2\psi_{11}}{\partial r\partial\theta}\right)_{r=1}. \tag{47}$$

The outer boundary layer has thickness of $O(R_s^{-1/2})$ which leads to the classical scaling

$$r-1 = R_s^{-1/2}\lambda, \qquad \psi_{20} = R_s^{-1/2}\tilde{\psi}_{20}. \tag{48}$$

In terms of the stream function and vorticity, defined as $\boldsymbol{\omega} = (0,0,-\nabla^2\psi)$, we then have, from Equations (41), (43) and (45),

$$\left(\left.V_\theta^d\right|_{r=1} + v_{20\theta}\right)\frac{\partial\tilde{\omega}_{20}}{\partial\theta} + \left(\left.\frac{\partial V_r^d}{\partial r}\right|_{r=1}\lambda + v_{20\lambda}\right)\frac{\partial\tilde{\omega}_{20}}{\partial\lambda} = \frac{\partial^2\tilde{\omega}_{20}}{\partial\lambda^2}, \tag{49}$$

$$\frac{\partial^2\tilde{\psi}_{20}}{\partial\lambda^2} = -\tilde{\omega}_{20}, \tag{50}$$

where

$$v_{20\theta} = -\frac{\partial\tilde{\psi}_{20}}{\partial\lambda}, \qquad v_{20\lambda} = \frac{\partial\tilde{\psi}_{20}}{\partial\theta}. \tag{51}$$

We note in (49) that, as with all unsteady flows of orbital type, the convective velocity for the vorticity is the Lagrangian mean velocity.

Equations (49) and (50) must be solved subject to a periodicity condition with period 2π in θ. In addition we require, at $\lambda = 0$,

$$\tilde{\psi}_{20} = 0, \qquad v_{20\theta} = -\frac{\partial \Psi_{20}}{\partial \rho}\bigg|_{\rho=\infty} = -c_{20}(\theta) = V_i, \tag{52}$$

say, where c_{20}, and so V_i, is determined uniquely by (37). A condition on $\tilde{\omega}_{20}$ at $\lambda = 0$ is determined from the 'slip' velocity at the inner edge of the boundary layer. At the outer edge, as $\lambda \to \infty$, we require

$$\tilde{\omega}_{20} \to 0, \qquad v_{20\theta} \to -\frac{\partial \psi_{20}}{\partial r}\bigg|_{r=1} = V_o, \text{ say.} \tag{53}$$

As we have already noted in Section 2.1 above the potential ϕ_{20}, and hence the stream function ψ_{20} derived from it, is not determined uniquely. The steady streaming outside the boundary layer, represented by ψ_{20}, may be augmented by the presence of a line vortex within the cylinder that induces a circulation about it. The circulation itself cannot be determined by inviscid means, and is chosen to ensure that $\tilde{\omega}_{20}$ approaches zero sufficiently smoothly at the edge of the boundary layer. The manner in which this is achieved is described in the next section.

With the circulation about the cylinder determined, so that the inviscid flow outside the boundary layer is given uniquely, the solution may be completed by an analysis of the flow at the bed $y = -H$. The analysis for the flow in the boundary layer in this region follows that above, up to the analogue of (49), (50) when we now have

$$(V_x^d|_{y=-H} + v_{20x})\frac{\partial \overline{\omega}_{20}}{\partial x} + \left(\frac{\partial V_y^d}{\partial y}\bigg|_{y=-H} Y + v_{20Y}\right)\frac{\partial \overline{\omega}_{20}}{\partial Y} = \frac{\partial^2 \overline{\omega}_{20}}{\partial Y^2}, \tag{54}$$

$$\frac{\partial^2 \overline{\psi}_{20}}{\partial Y^2} = -\overline{\omega}_{20}, \tag{55}$$

where

$$v_{20x} = \frac{\partial \overline{\psi}_{20}}{\partial Y}, \qquad v_{20Y} = -\frac{\partial \overline{\psi}_{20}}{\partial x}, \tag{56}$$

and

$$y + H = R_s^{-1/2} Y, \qquad \psi_{20} - \psi_{20}|_{y=-H} = R_s^{-1/2}\overline{\psi}_{20}. \tag{57}$$

The boundary conditions require

$$\overline{\psi}_{20} = 0, \qquad v_{20x} = \overline{c}_{20}(x) = \overline{V}_i, \quad \text{at } Y = 0, \tag{58}$$

$$\overline{\omega}_{20} \to 0, \qquad v_{20x} \to \frac{\partial \psi_{20}}{\partial y}\bigg|_{y=-H}, \quad \text{as } Y \to \infty. \tag{59}$$

In (54) V_x^d, V_y^d are the x, y components of the Stokes drift velocity, $\overline{c}_{20} = \overline{c}_{20}(x)$ in (58) is determined from the steady streaming velocity at the edge of the Stokes layer on the bed as

$$\begin{aligned}\overline{c}_{20}(x) &= \tfrac{3}{2}(c_{11}c'_{12} - c_{12}c'_{11}) - \tfrac{3}{2}(c_{11}c'_{11} + c_{12}c'_{12}) \\ &= -\frac{3}{4}\left\{\frac{\partial\psi_{11}}{\partial y}\left(\frac{\partial^2\psi_{11}}{\partial x\partial y} - \frac{\partial^2\psi_{12}}{\partial x\partial y}\right) + \frac{\partial\psi_{12}}{\partial y}\left(\frac{\partial^2\psi_{11}}{\partial x\partial y} + \frac{\partial^2\psi_{12}}{\partial x\partial y}\right)\right\}_{y=-H}, \end{aligned} \tag{60}$$

and ψ_{20} in (59) is of course, uniquely determined from the boundary-layer analysis at $r = 1$.

3. Numerical considerations

The numerical techniques we have used are based on those described by Riley and Yan [3] and Yan and Riley [4]. For the potentials ϕ_{11}, ϕ_{12} and ϕ_{20} the Boundary Element method used in [3] is again employed, with the only difference that $\partial\phi_{ij}/\partial y = 0$ on $y = -H$ replaces the vanishing of $\partial\phi_{ij}/\partial y$ as $y \to -\infty$. Full details of this method are given in [3], and are not repeated here.

The solution derived for ϕ_{20}, and hence ψ_{20}, is devoid of circulation. This must be augmented by a potential function ϕ_v, or ψ_v, to account for circulation (and it is the augmented ψ_{20} that appears in Equations (53) and (59)). Consider the quantity ψ_v, this satisfies

$$\nabla^2\psi_v = 0 \tag{61}$$

with

$$\psi_v = 0, \quad \text{on } y = h, -H, \tag{62}$$

$$\psi_v \to 0, \quad \text{as } x \to \pm\infty, \tag{63}$$

$$\psi_v = C, \quad \text{on } r = 1. \tag{64}$$

We work in the finite domain $-H \leqslant y \leqslant h$, $x_l \leqslant x \leqslant x_r$ where, typically, $-x_l = x_r = 50$ or four times the wave length; the conditions as $x \to \pm\infty$ are then replaced by

$$\frac{\partial\psi_v}{\partial x} - \frac{\pi}{h+H}\psi_v = 0, \quad \text{on } x = x_l, \qquad \frac{\partial\psi_v}{\partial x} + \frac{\pi}{h+H}\psi_v = 0, \quad \text{on } x = x_r. \tag{65}$$

Equation (61), together with (62), (64) and (65) is then solved again, by means of the Boundary Element method described in [3]. The choice of C, which determines the circulation, depends upon a consideration of the viscous problem defined by (49) to (53), as we now discuss.

To integrate the boundary-layer equations (49) to (53) on the cylinder we use, as in [4], a standard finite-difference technique in which derivatives in the streamwise direction are represented by second-order-accurate upwind differences, whilst cross-stream derivatives are represented by central differences. For the cases considered the mesh sizes in the discretized equations varied with $\delta\theta$ in the range $\pi/60$ to $\pi/40$ and $\delta\lambda$ in the range 0·05 to 0·1. For smaller values of h and H a finer mesh was used, in general. For each case considered we choose a value of λ_∞, to represent the edge of the boundary layer, in the range 10 to 15. For a given value of the constant C in (64), from which the circulation is easily determined, it is possible, following a suitable number of sweeps in the boundary layer, to establish a periodic solution.

Periodicity, therefore, plays no part in determining a unique value for C. It is the boundary condition (53) for $\tilde{\omega}_{20}$ that is crucial in this respect. Implicit in the condition that $\tilde{\omega}_{20}$ vanishes as $\lambda \to \infty$, is the requirement that all of its cross-stream derivatives also vanish. If we define

$$I(C, \lambda_\infty) = \int_0^{2\pi} \left| \frac{\partial \tilde{\omega}_{20}}{\partial \lambda} \right|_{\lambda=\lambda_\infty} \mathrm{d}\theta, \tag{66}$$

then, see [4, 8], we may expect that for a given value of λ_∞, I will pass through a minimum for some critical value of C, say C_c, and that as λ_∞ increases C_c will become more sharply defined. In this way we are able to make an accurate estimate of C_c, and hence the circulation about the cylinder.

With the circulation so determined, there remains the outer boundary layer at the bed $y = -H$. The main difference between this, and the corresponding boundary layer on the cylinder, is that the latter is periodic. The dominant influence on the bed boundary layer is the outer flow. This is in the direction of x decreasing, and the pressure gradient associated with it is impressed upon the boundary layer. This outer flow accelerates until it passes beneath the cylinder, thereon it decelerates. At the inner edge of this outer boundary layer there is a small region, in $x \geqslant 0$, where the flow is in the positive x-direction. For most cases the small region of reversed flow is unimportant, and it is possible to calculate the boundary-layer flow by standard marching procedures from $x = x_r$, say, where, typically, $x_r = 15$. However in cases where the bed is close to the cylinder, the velocities at the inner and outer edges of the outer boundary layer may be of comparable magnitude. In that case a marching procedure cannot be expected to succeed and we have treated the problem as a boundary-value problem in $x_l \leqslant x \leqslant x_r$ where $-x_l = x_r$. Such a method must, however, be used with caution on account of the singularity that is known to develop in the solution of the boundary-layer equations at separation. In our calculations we have taken Y_∞, the edge of the boundary layer, to be in the range 10 to 15 with δx and δY each in the range 0·05 to 0·1.

In the next section we discuss the results we have obtained by the methods described above.

4. Results and discussions

As we have already indicated, our main concern is with the time-averaged properties of the flow. In particular we are interested in the effect of finite depth on the flow about the cylinder, and the nature of the flow at the bed $y = -H$ itself. We limit our investigation to the single wave number $k = 0{\cdot}5$, and we consider first the inviscid-flow problem.

The Boundary-Element method has been employed, as described in [3]. Based on our experience, as discussed in [3], if we take a typical case with $-x_l = x_r = 50$, which is about four times the wavelength for $k = 0{\cdot}5$, then the number of elements on the cylinder $N_1 = 120$, on the bed $y = -H$, $N_2 = 600$, on the free surface $N_3 = 600$, and on $x = x_l, x_r$, $N_{4,5} = 140$. The boundary conditions for the unknown potentials are set out in Equations (17) to (22). Before any consideration of the time-averaged flow, determined at the second order, we examine the free-surface profile.

Equations (24), with the leading-order term of (23), determine the free surface at $O(\epsilon)$ whilst η_{20} in (25) provides the time-averaged displacement of the free surface, correct to $O(\epsilon^2)$, and we note that this is determined in terms of the leading-order potentials. For liquid of infinite depth it has long been established [5, 6] that at leading order there is no reflected wave, and more recently [3, 7] that this is also true at second order. However, when the circular

Table 1. The appropriate unique values of the circulation, Γ_c, for various values of H and h, in the case $k = 0{\cdot}5$.

$H \backslash h$	2	4	6
1·3	−1·66	−0·127	−0·02
1·5	−3·18	−0·162	−0·0225
2·0	−6·40	−0·672	−0·0253

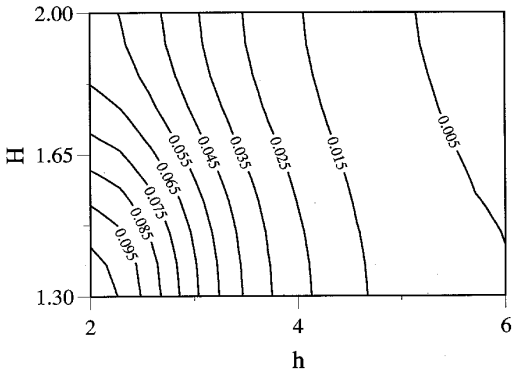

Figure 2. The variation of the reflected wave amplitude coefficient R with h and H for $k = 0{\cdot}5$.

cylinder is placed beneath waves in liquid of finite depth this is no longer true, and there is a reflected wave in $x < 0$. If we denote the amplitude of this reflected wave by ϵR then from (23) and (24) we have at first order,

$$R = \Omega(\phi_{11}^2 + \phi_{12}^2)_{y=h}^{1/2}. \tag{67}$$

The dependence of this reflected wave amplitude coefficient on h and H is shown in Figure 2. As may be expected, it increases as the cylinder depth, and the total water depth, decrease. From Equations (23) and (25) we see that the mean surface elevation, η_{20}, is also determined when the leading-order potentials are known. Examples are shown in Figure 3. What we see, in all cases, is that ahead of the cylinder the time-averaged surface elevation takes the form of a small amplitude stationary wave, whilst behind the cylinder it is almost uniform. This contrasts with the case of infinite depth, where on average the free surface is depressed over the cylinder. However, as H increases the time-averaged free surface approaches that shown in Figure 8(a) of [3].

We turn next to the steady streaming at $O(\epsilon^2)$. The potential ϕ_{20}, obtained using conditions (18) to (22), is devoid of circulation about the cylinder. But as we have already indicated the solution is not unique. To it we can add the potential of a line vortex within the cylinder, that results in a circulation about it. In [4], where the liquid depth is assumed to be infinite, a relatively simple analytic representation of the circulatory flow is introduced. The present situation is more complex, and in Equations (61) to (64) we have posed the problem for the circulatory stream function ψ_v. For a given C in (64), the circulation Γ about the cylinder may be easily determined. The question to be answered is, how is Γ to be uniquely determined? The answer to this question follows a consideration of viscous effects. We are interested in situations for which $R_s \gg 1$, and so viscous effects are confined to thin boundary layers adjacent to the cylinder and bed. Following Yan and Riley [4], based on an earlier idea of Riley [8], we see that the outer boundary layer on the cylinder surface will only match satisfactorily with the Stokes layer, and the outer inviscid flow, for a value of Γ that has to be determined numerically. The manner in which this is achieved has been described in Section 3. For an example of how this works in practice we refer the reader to Figure 5 of [4]. In Table 1 we set out the appropriate unique values of the circulation, Γ_c, for the case $k = 0{\cdot}5$ and various values of H and h. In Figure 4 we show the time averaged streamlines for a subset of the results set out in Table 1. If ψ_s denotes the stream function for the steady streaming then

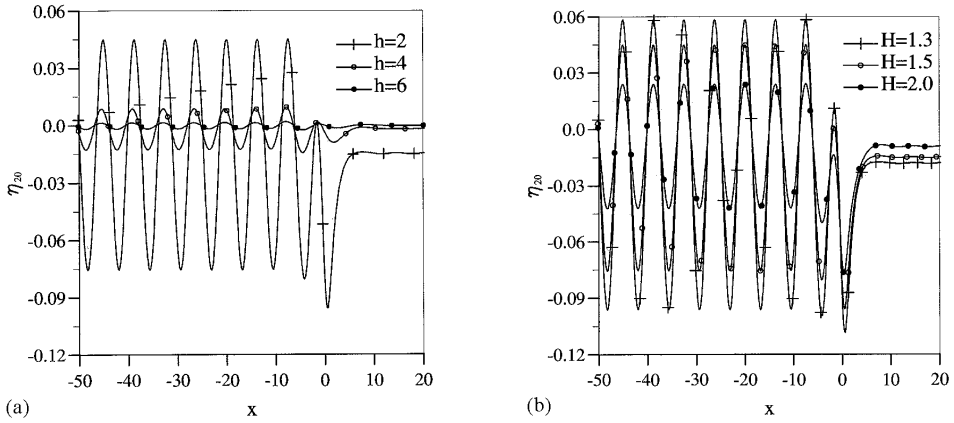

Figure 3. The time-averaged free surface profile η_{20} for $k = 0{\cdot}5$, (a) $H = 0{\cdot}5$, (b) $h = 2$.

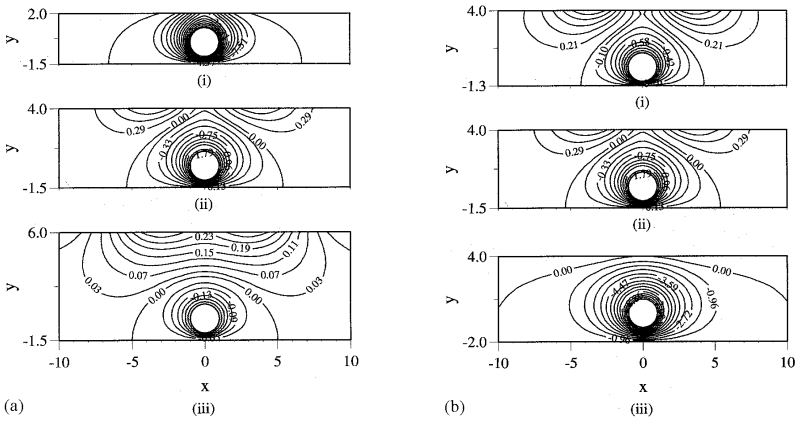

Figure 4. The development of the inviscid steady streaming for $k = 0{\cdot}5$, (a) for $H = 1{\cdot}5$, and (i) $h = 2$, (ii) $h = 4$, (iii) $h = 6$; (b) for $h = 4$, and (i) $H = 1{\cdot}3$, (ii) $H = 1{\cdot}5$, (iii) $H = 2{\cdot}0$.

$\psi_s = \psi_{20} + \psi_v =$ constant determines these time-averaged streamlines. Figure 4(a) shows the development of the inviscid steady streaming as h increases, with the gap between the cylinder and the bed fixed. As the depth increases the circulatory nature of the flow remains confined to the neighbourhood of the cylinder, whilst towards the surface conditions are clearly more influenced by free-surface effects. The flow between the cylinder and bed, which is in the negative x-direction, diminishes as h increases along with the circulation. Figure 4(b) shows the inviscid time-averaged streamlines when the cylinder is at a fixed depth, but the gap between it and the bed decreases. When the cylinder is close to the bed the circulation is small, it must vanish in the limit as the gap vanishes, and the flow between cylinder and bed is weak. But as the gap increases it is clear that the circulatory flow about the cylinder has a profound effect upon the mean streamlines, and a much stronger flow is induced between the cylinder and the bed.

Consider now the steady boundary layers on the cylinder and bed. First, in Figure 5, we present the velocities at the inner and outer edges of the outer boundary layer on the cylinder.

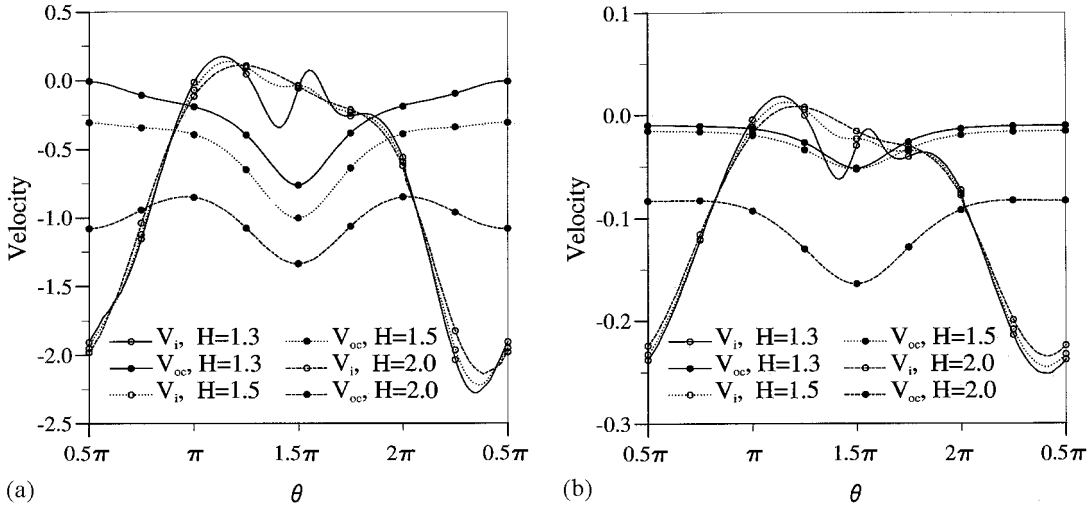

Figure 5. Velocities at the inner and outer edges of the outer boundary layer on the cylinder for $k = 0{\cdot}5$, (a) $h = 2$, (b) $h = 4$.

These are the velocities that drive the boundary-layer flow. Both Figure 5(a) and 5(b) refer to the case $k = 0{\cdot}5$. The first point to note is that doubling the cylinder depth beneath the free surface reduces these velocities by an order of magnitude, as may perhaps be expected. Otherwise there are similarities between them. Consider first V_i, the velocity at the edge of the Stokes layer defined by Equation (52); this is the inner boundary condition for the outer boundary layer. For all three cases shown V_i is very similar over most of the cylinder surface, except as the gap closes we note the variations close to $\theta = \frac{3}{2}\pi$ where the cylinder is closest to the bed. The velocity at the outer edge of this boundary layer is made up of two parts. First we have V_o, defined by equation (53), but, as we have noted, there is another contribution to augment this as the velocity at the outer edge of our outer boundary layer due to circulation about the cylinder. The complete outer velocity we have denoted by V_{oc} in Figure 5. This outer velocity is characterised, in all cases, by its extremum value at $\theta = \frac{3}{2}\pi$. The velocities V_i and V_{oc} are comparable in order of magnitude, but their greatly differing variations with θ emphasise the need for this outer boundary layer. In Figure 6 we give an example showing the tangential velocity component in the boundary layer, as it accommodates the velocities at its edges, at various stations. This may be considered as a typical case, and clearly shows how the boundary layer accommodates the inviscid velocity of slip at its outer edge and velocity of slip generated by the Stokes layer at its inner edge.

Finally, we consider the boundary layer on the bed $y = -H$. Again, now in Figure 7, we show the velocities that drive our boundary layer on the bed namely V_i at the edge of the Stokes layer, and V_{oc} from the outer inviscid flow, for the six cases under consideration. As with the corresponding velocities at the cylinder surface, these reduce by an order of magnitude as the depth of the cylinder beneath the free surface doubles. But in each case the velocities follow a similar pattern. Consider first a typical distribution of V_i. What we see is that there is a divergence of flow at the edge of the Stokes layer immediately below the cylinder, which decays within a cylinder diameter. Furthermore, as the distance between the cylinder and bed increases this velocity decreases in amplitude. By contrast the slip

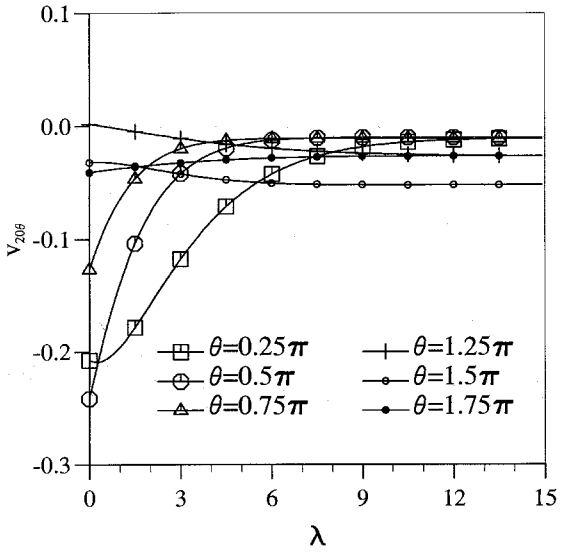

Figure 6. The tangential velocity component in the outer boundary layer on the cylinder for $k = 0{\cdot}5$, $h = 4$ and $H = 1{\cdot}3$.

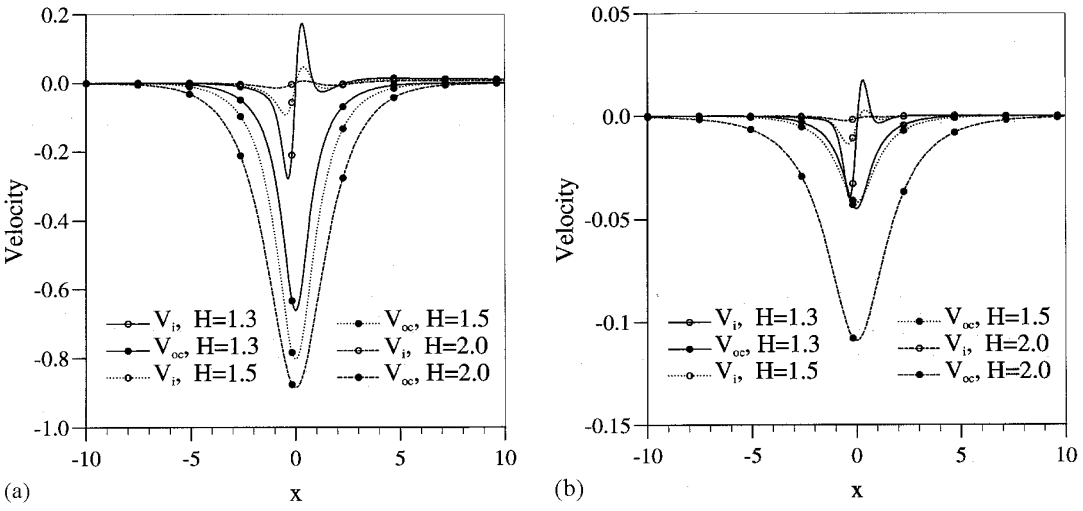

Figure 7. Velocities at the inner and outer edges of the outer boundary layer on the bed for $k = 0{\cdot}5$, (a) $h = 2$, (b) $h = 4$.

velocity V_{oc}, at the outer edge of the outer boundary layer, determined from the outer inviscid flow, is uni-directional. It is dominated by the circulation about the cylinder, resulting in a velocity of slip in the direction of x decreasing which reaches a peak immediately beneath the cylinder. Furthermore, as we see, the amplitude of this velocity increases as the distance, H, between cylinder and bed increases. This outer flow also impresses a pressure gradient on the boundary layer that is favourable for $x > 0$, and adverse for $x < 0$. The dynamics of this outer boundary layer, determined by various competing influences are not, therefore, entirely straightforward. What we have found, from integration of the boundary-layer equations, is

that the outer inviscid flow with its attendant pressure gradient is a dominant influence. From the cases illustrated in Figure 7 only those for which $h = 4, H \leqslant 1{\cdot}5$ yield a boundary layer that maintains its integrity as we move from large positive, to negative, values of x. Both of these cases are characterised by a relatively weak outer streaming. In all the other cases considered, which must therefore be considered typical, the adverse pressure gradient stimulates flow separation, characterised by the development of a singularity in the solution of the boundary-layer equations, within one cylinder diameter downstream from the velocity peak. We have not considered the consequences of such flow separation on the outer inviscid flow.

If the bed over which the flow we have considered is mobile or erodible, for example sand, then it is important to understand how it will respond to the flow described above. When a particulate bed is subjected to intense shear then Acrivos (private communication) has shown that, in a direction *normal* to the shear stress, the solid particles are subject to diffusion, and estimates may be made of the diffusion coefficient. In the present situation the dominant shear stress at the boundary is provided by the leading-order Stokes-layer fluctuations. We postulate that diffusion normal to the bed will lead to migration of solid particles away from it, that they will ultimately find themselves in the region we have identified as the outer boundary layer, and be transported by the flow-field therein. This will lead to an erosion of the bed immediately beneath the cylinder, with bed material transported in the direction of x decreasing. The extent to which this is transported will, of course, depend upon whether or not flow separation takes place. But the distributions of V_{oc} shown in Figure 7 suggest that this cannot be expected to exceed about five cylinder diameters. Support for the mechanism outlined above for the transport of bed material is provided by the experiments reported by Wybrow, Yan and Riley [1], and Wybrow and Riley [2]. In those investigations standing waves provided flow structures in which, as here, a Stokes layer, within which steady streaming originates, is embedded within an outer steady-streaming boundary layer. In experiments carried out to support the theory, a fine coating of small glass beads covered the surfaces over which the streaming took place. The subsequent migration of these tiny particles, average diameter 50μ, was in all case consistent with streaming predicted in the outer boundary layer.

Acknowledgement

The authors are indebted to the Marine Technology Directorate for financial support.

References

1. M.F. Wybrow, B. Yan and N. Riley, Oscillatory flow over a circular cylinder close to a plane boundary. *Fluid Dyn. Res.* 18 (1996) 269–288.
2. M.F. Wybrow and N. Riley, Oscillatory flow over a cylinder resting on a plane boundary. *Eur. J. Appl. Math.* (1996) 545–558.
3. N. Riley and B. Yan, Inviscid fluid flow around a submerged circular cylinder induced by free-surface travelling waves. *J. Eng. Math.* 30 (1996) 587–601.
4. B. Yan and N. Riley, Boundary-layer flow around a submerged circular cylinder induced by free-surface travelling waves. *J. Fluid Mech.* 316 (1996) 241–257.
5. W.R. Dean, On the reflexion of surface waves by a submerged circular cylinder. *Proc. Camb. Phil. Soc.* 44 (1948) 483–491.
6. F. Ursell, Surface waves on deep water in the presence of a submerged circular cylinder. I. *Proc. Camb. Phil. Soc.* 46 (1950) 141–152.
7. M. McIver and P. McIver, Second-order wave diffraction by a submerged circular cylinder. *J. Fluid Mech.* 219 (1990) 519–529.
8. N. Riley, High Reynolds number flows with closed streamlines. *J. Eng. Math.* 15 (1981) 15–27.